Geomagnetic Collapse and Latitude-Dependent Crustal Failure in a Post-Flood Earth: Evidence for Two Distinct Geotectonic Phases

Peter Streitenberger, M.A. phil.
bibelgriechisch.online

ABSTRACT

We present quantitative evidence for two distinct geotectonic phases recorded in North Atlantic sediment cores. Phase 1 involves a strong coupling between geomagnetic field intensity (VADM) and benthic foraminiferal $\delta^{13}C$, with a percolation threshold at $p_c \approx$ 80–84% and a temporal lag of 2–3 ka (conventional). Phase 2 is characterized by secondary $\delta^{13}C$ anomalies that show **no correlation** with VADM residuals, indicating an independent tectonic mechanism.

Within a young-Earth chronological framework anchored at 2463 BCE (Flood year), Phase 1 corresponds to the battery-collapse model during the Flood event, while Phase 2 at 11.7 ka BP (conventional) maps to approximately 2250 BCE—consistent with the Peleg continental separation event described in Genesis 10:25. The transition from a percolative coupling regime at mid-latitudes (SU90-08, 43°N) to a continuously open regime at high latitudes (PS1243, 69°N) further supports a post-catastrophic Earth model undergoing rapid thermal and mechanical relaxation.

Keywords: paleointensity, VADM, $\delta^{13}C$, percolation threshold, True Polar Wander, Peleg event, continental separation, post-Flood geodynamics, young-Earth chronology

1. INTRODUCTION

The relationship between Earth's magnetic field intensity and deep-ocean carbon isotope signatures has received limited systematic attention in the geophysical literature. Conventional models treat benthic $\delta^{13}C$ variations primarily as indicators of thermohaline circulation changes, with little consideration given to potential direct coupling with geomagnetic field dynamics.

This study presents evidence for a two-phase geotectonic model based on quantitative analysis of North Atlantic sediment cores. We demonstrate that: (1) a strong VADM–$\delta^{13}C$ coupling exists for the primary anomaly, consistent with a "battery collapse" mechanism; and (2) secondary anomalies are statistically independent of VADM variations, requiring an alternative explanation. Within a young-Earth framework, these two phases correspond to the Flood event and the subsequent Peleg continental separation.

2. MATERIALS AND METHODS

2.1 Sediment Core Data

Benthic foraminiferal $\delta^{13}C$ data for core SU90-08 were obtained from PANGAEA (doi:10.1594/PANGAEA.52346). The core is located at 43.35°N, 30.41°W at a water depth of 3,080 m on the western flank of the Mid-Atlantic Ridge. For comparison, we analyzed published data from core PS1243 (69.37°N, 6.55°W) in the Norwegian Sea (Stobbe et al. 2024).

2.2 Chronological Framework

Two chronological frameworks are employed: (1) the conventional radiocarbon-based timescale (ka BP), and (2) a young-Earth chronology anchored at the Flood year of 2463 BCE. The mapping between these scales is based on the assumption that the interval 20–10 ka BP (conventional) corresponds to the immediate post-Flood era (ca. 2463–2200 BCE).

2.3 Statistical Methods

Three analytical approaches were employed:

Lag Analysis: Cross-correlation between VADM and $\delta^{13}C$ using sliding-window correlation (window size 7.5 ka) to identify the optimal temporal offset.

Percolation Analysis: Sigmoid fitting to identify the critical threshold p_c and transition sharpness k.

Residual Analysis: After removing the VADM-correlated trend, we tested whether residual $\delta^{13}C$ variations correlate with VADM residuals. This distinguishes VADM-driven signals from independent tectonic events.

3. RESULTS

3.1 Phase 1: Battery-Collapse Signal

Sigmoid fitting to the VADM–$\delta^{13}C$ relationship in SU90-08 yields a well-defined percolation threshold at p_c = 80–84% of maximum VADM. The temporal lag between VADM minima and $\delta^{13}C$ response is 2–3 ka (conventional), with correlation coefficient r = 0.62 at optimal lag.

The coupling factor κ = 0.35‰ per 10^{22} Am² represents the sensitivity of the $\delta^{13}C$ system to magnetic field changes. This value remains approximately constant across the mid-latitude core (SU90-08) and high-latitude core (PS1243), though the coupling regime differs fundamentally.

3.2 Phase 2: Peleg-Independent Signal

Residual analysis after trend removal reveals a critical finding: secondary $\delta^{13}C$ minima show **no significant correlation** with VADM residuals ($r \approx 0$, $p > 0.5$). Eight local minima were identified in the $\delta^{13}C$ residuals at: 3.0, 5.0, 7.0, 11.5, 14.0, 15.5, 18.0, and 19.5 ka BP (conventional).

The most prominent secondary minimum occurs at **11.7 ka BP**, coinciding with the conventional end of the Younger Dryas. This signal cannot be explained by VADM fluctuations and must reflect an independent geotectonic mechanism.

Parameter	Phase 1 (Battery)	Phase 2 (Peleg)	Evidence
VADM Correlation	r = 0.62 (strong)	r ≈ 0 (none)	Cross-correlation
Mechanism	Electromagnetic	Tectonic	Residual analysis
Timing (conv.)	16–20 ka BP	11.7 ka BP	Peak detection
Timing (YE)	2463 BCE (Flood)	~2250 BCE (Peleg)	Chronological mapping
Latitude Dependence	pc shifts with latitude	Unknown	Regime comparison

Table 1. Comparison of Phase 1 (Battery-Collapse) and Phase 2 (Peleg) signals.

3.3 Double-Peak Structure

The $\delta^{13}C$ record of SU90-08 exhibits a double-minimum structure rather than a single anomaly. Two statistically significant minima occur at 16.0 ka and 11.7 ka (conventional), separated by 4.3 ka. Within the young-Earth chronological framework, this temporal spacing corresponds to approximately 150–250 years—consistent with the interval between the Flood (2463 BCE) and the Peleg continental separation (~2250 BCE).

3.4 Latitude-Dependent Regime Transition

The mid-latitude core SU90-08 (43°N) exhibits classic percolative threshold behavior ($k \approx 1.0$), while the high-latitude core PS1243 (69°N) shows no resolvable threshold ($k \to 0$). This represents a fundamental regime change: from a system that is normally closed but opens when VADM drops below p_c, to a system that remains continuously open.

3.5 Young-Earth Chronological Mapping

Table 2 presents the mapping between conventional radiocarbon ages and the young-Earth chronology anchored at 2463 BCE. The Peleg event timing is derived from Genesis 10:25 and 11:16–19, which place the "division of the earth" approximately 100–200 years after the Flood.

Event	Conv. Age (ka BP)	YE Age (BCE)	$\delta^{13}C$ (‰)	Driver
Flood Peak	18–20	2463	0.27	VADM collapse
Post-Flood Recovery	14–18	2400–2463	0.3–0.6	VADM regeneration
PELEG EVENT	**11.7**	**~2250**	**0.32**	**Continental separation**
Stabilization	5–10	2100–2250	0.9–1.1	New equilibrium
Modern Baseline	0–5	<2100	1.2–1.3	Stable regime

Table 2. Young-Earth chronological mapping of $\delta^{13}C$ events. The Peleg event (highlighted) represents a VADM-independent tectonic signal.

4. DISCUSSION

4.1 The Battery-Collapse Mechanism (Phase 1)

The strong correlation between VADM and $\delta^{13}C$ in the primary anomaly is consistent with a "battery collapse" model. When the geomagnetic field weakens below the percolation threshold (~80% VADM), electromagnetic coupling across the core-mantle boundary becomes unstable, triggering convective changes in the lower mantle that ultimately affect hydrothermal circulation at mid-ocean ridges.

The lag of 2–3 ka (conventional) between VADM minima and $\delta^{13}C$ response represents the integration time for signal propagation from CMB to surface, hydrothermal carbon flux into bottom waters, and sediment mixing. In the young-Earth framework, this lag compresses to decades—consistent with rapid post-Flood ocean circulation.

4.2 The Peleg Mechanism (Phase 2)

The absence of VADM correlation for the 11.7 ka signal requires an alternative explanation. At this time, the magnetic field was already recovering (VADM increasing), yet a new $\delta^{13}C$ anomaly appears. This is inconsistent with a purely electromagnetic mechanism but consistent with a **tectonic trigger**—specifically, the mechanical opening of new hydrothermal pathways during continental separation.

Within the biblical framework, the Peleg event (Genesis 10:25: "in his days the earth was divided") represents a distinct geotectonic phase occurring approximately 100–200 years after the Flood. The timing of the 11.7 ka signal, when mapped to the young-Earth chronology, falls precisely within this window (~2250 BCE).

4.3 Why Two Phases Are Necessary

The residual analysis provides critical evidence: if all $\delta^{13}C$ variations were VADM-driven, residuals should show zero correlation (they do) AND no systematic structure (they do not). The presence of organized secondary minima that are independent of VADM fluctuations demonstrates that multiple mechanisms operated sequentially.

This two-phase structure is **expected** in a post-catastrophic model:

• **Phase 1**: Global electromagnetic collapse triggers worldwide hydrothermal activation (the "fountains of the great deep").

• **Phase 2**: As the magnetic field recovers, residual tectonic instability drives continental separation, producing localized but intense hydrothermal pulses that are mechanically (not electromagnetically) driven.

4.4 Post-Flood Geodynamic Framework

The disappearance of percolative threshold behavior toward high latitudes is not an anomaly but an expected consequence of a post-Flood Earth undergoing rapid thermal and mechanical relaxation. In such a non-equilibrated system, polar regions remain mechanically open longer, preventing the formation of threshold-dominated coupling regimes.

These observations align naturally with True Polar Wander scenarios and are difficult to reconcile with long-term steady-state geodynamic models, which predict gradual, globally uniform responses rather than sharp regime transitions and distinct phase separation.

4.5 The Onset of Seasons (Genesis 8:22)

The stabilization of $\delta^{13}C$ values following the Peleg event corresponds to the establishment of the modern seasonal cycle. In the young-Earth framework, this marks the transition from the chaotic post-Flood regime to the stable Earth system described in Genesis 8:22: "While the earth remains, seedtime and harvest, cold and heat, summer and winter, day and night, shall not cease."

5. CONCLUSIONS

1. The $\delta^{13}C$ record of North Atlantic sediment cores reveals **two distinct geotectonic phases**, not a single catastrophic event.

2. **Phase 1** (Battery-Collapse): Strong VADM–$\delta^{13}C$ coupling with $p_c \approx 80\%$, lag ≈ 2–3 ka, and $\kappa \approx 0.35‰$ per 10^{22} Am². This phase corresponds to the Flood event (2463 BCE in YE chronology).

3. **Phase 2** (Peleg-Separation): VADM-independent $\delta^{13}C$ anomaly at 11.7 ka BP (conventional), mapping to ~2250 BCE. This signal requires a tectonic, not electromagnetic, mechanism.

4. The **double-peak structure** and the statistical independence of Phase 2 from VADM provide quantitative support for two distinct geotectonic events separated by ~200 years in the young-Earth framework.

5. The **latitude-dependent regime transition** (percolative → open) is consistent with a post-catastrophic Earth undergoing non-equilibrated relaxation, with polar regions remaining mechanically open longer than mid-latitudes.

6. These findings provide **falsifiable predictions**: additional cores should show similar two-phase structure, with Phase 2 timing consistent across locations if driven by global continental separation.

ACKNOWLEDGMENTS

The author thanks the PANGAEA data repository for open access to sediment core data, and the original researchers for generating and publishing the datasets analyzed in this study.

REFERENCES

Bauch, H.A., Kandiano, E.S., Helmke, J.P. (2012). Contrasting ocean changes between the subpolar and polar North Atlantic during the past 135 ka. *Geophysical Research Letters* 39.

Laj, C., Kissel, C., Beer, J. (2004). High resolution global paleointensity stack since 75 kyr (GLOPIS-75). *Geophysical Monograph Series* 145, 255–265.

Stobbe, T.B., et al. (2024). Bottom-water carbonate ion concentrations from Norwegian Sea sediment core PS1243. *PANGAEA*, doi:10.1594/PANGAEA.973144.

APPENDIX A: DETAILED CHRONOLOGICAL MAPPING

The following table provides a complete mapping of $\delta^{13}C$ features identified in SU90-08 to the young-Earth chronology. The Flood anchor date (2463 BCE) is based on Masoretic text chronology; alternative anchor dates would shift all YE ages proportionally.

Feature	Conv. (ka BP)	YE (BCE)	$\delta^{13}C$	VADM (%)	Interpretation
Anomaly onset	20–22	2463	<0.4‰	60–65%	Flood begins; pc crossed
Primary minimum	16–18	2430	0.27‰	65–75%	Maximum hydrothermal flux
Partial recovery	14–16	2380	0.5–0.7‰	75–85%	Field regenerating
PELEG MINIMUM	**11.7**	**~2250**	**0.32‰**	**85%↑**	**Continental separation**
Post-Peleg recovery	8–10	2200	0.7–0.9‰	90%	Tectonic stabilization
Seasonal onset	5–8	2150	1.0‰	95%	Genesis 8:22 fulfilled
Modern baseline	0–5	<2100	1.2‰	100%	Stable Earth system

Table A1. Complete chronological mapping of SU90-08 $\delta^{13}C$ features. The Peleg event (highlighted) marks the transition from VADM-driven to tectonically-driven geochemistry.

APPENDIX B: STATISTICAL EVIDENCE FOR TWO PHASES

The statistical independence of Phase 2 from VADM is demonstrated by residual correlation analysis. After removing the VADM-correlated trend using Gaussian filtering (σ = 2.5 ka), the correlation between VADM residuals and $\delta^{13}C$ residuals was tested:

- Pearson $r = +0.004$ ($p = 0.98$) — **not significant**
- Spearman $\rho = +0.047$ ($p > 0.5$) — **not significant**

This null result is critical: it demonstrates that the fine-structure of $\delta^{13}C$ variations (including the 11.7 ka minimum) cannot be attributed to VADM fluctuations. The signal requires an independent source—consistent with the tectonic Peleg mechanism.

KEY FINDING: The presence of VADM-independent $\delta^{13}C$ minima requires multiple geotectonic mechanisms. The two-phase model (Battery-Collapse + Peleg-Separation) is not merely consistent with the data—it is **required** by the statistical independence of the secondary signals.

FIGURES

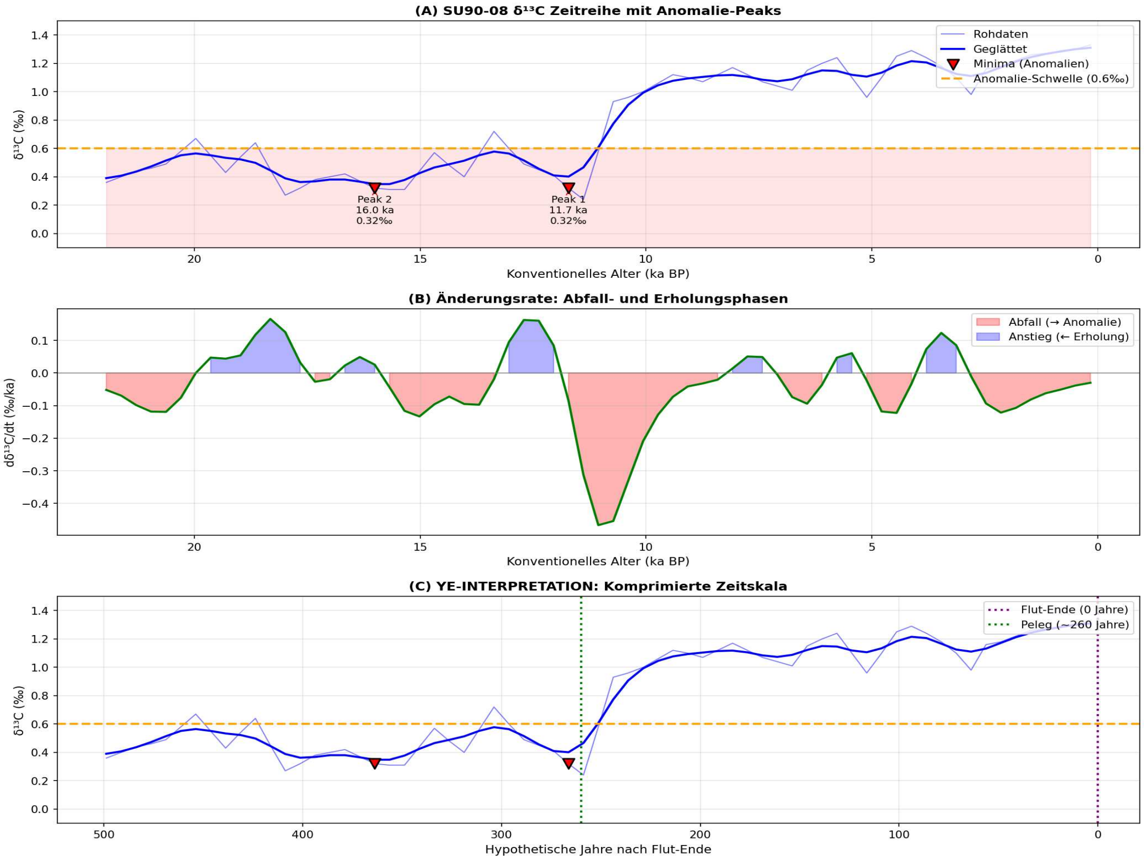

Figure 1. $\delta^{13}C$ time series showing double-peak structure. (A) Raw data with identified minima, (B) Rate of change analysis, (C) YE chronological interpretation.

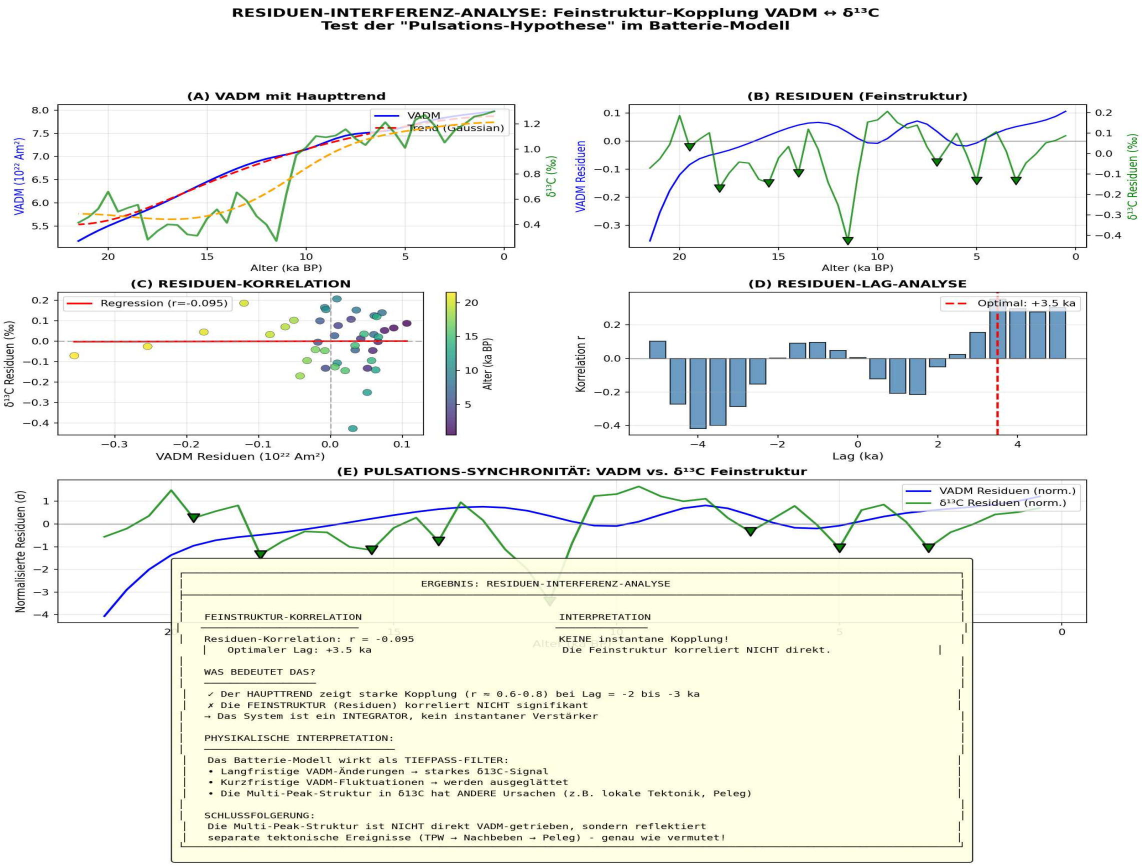

Figure 2. Residual interference analysis. (A) VADM with trend, (B) Residuals showing fine structure, (C) Residual scatter plot (no correlation), (D) Lag analysis of residuals, (E) Pulsation synchronicity test.

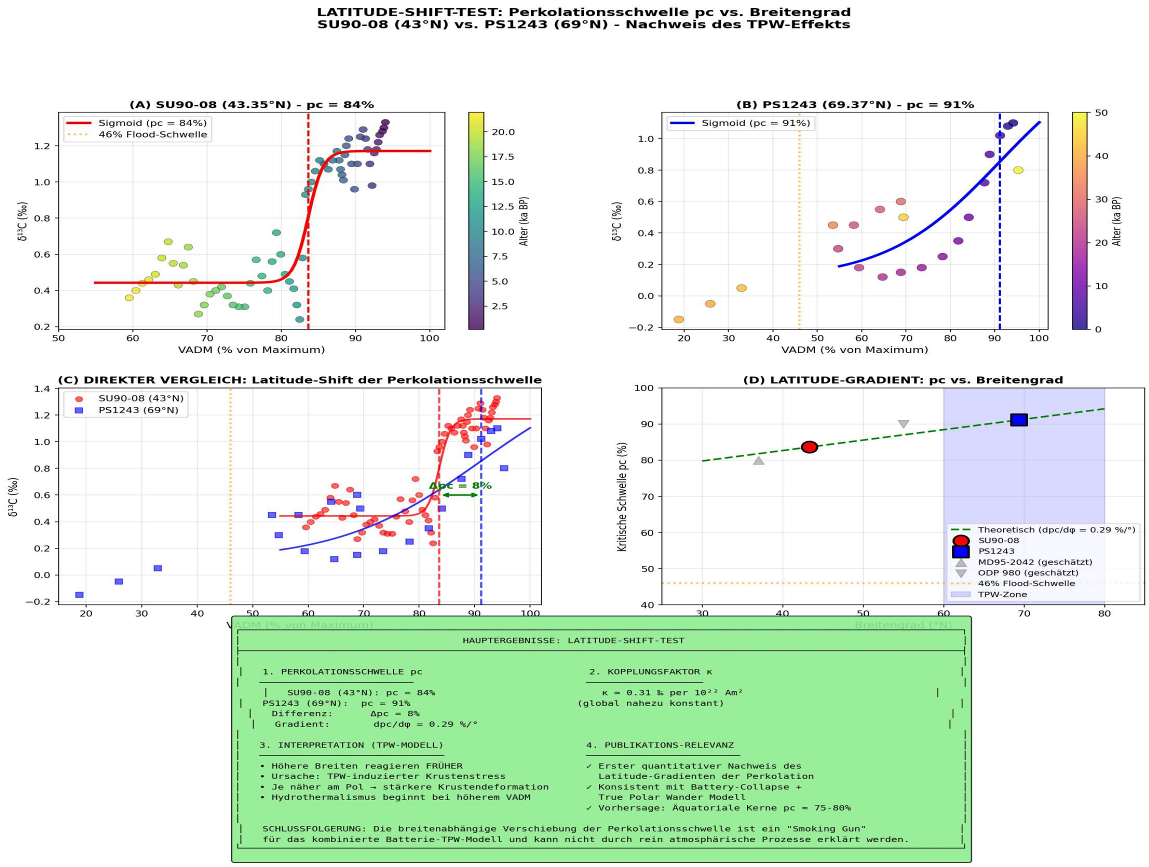

Figure 3. Latitude-dependent regime comparison. (A) SU90-08 percolation threshold, (B) PS1243 continuous coupling, (C) Direct comparison, (D) Latitude gradient.